Status of the ITER heating neutral beam system

To cite this article: R. Hemsworth *et al* 2009 *Nucl. Fusion* **49** 045006

Nucl. Fusion 49 (2009) 045006 (15pp) doi:10.1088/0029-5515/49/4/045006

Status of the ITER heating neutral beam system

R. Hemsworth[1], H. Decamps[1], J. Graceffa[1], B. Schunke[1], M. Tanaka[1], M. Dremel[1], A. Tanga[1], H.P.L. De Esch[2], F. Geli[3], J. Milnes[3], T. Inoue[4], D. Marcuzzi[5], P. Sonato[5] and P. Zaccaria[5]

[1] ITER Organization, 13108 St Paul lez Durance Cedex, Cadarache, France
[2] CEA, IRFM, F-13108 St Paul lez Durance France
[3] EURATOM/UKAEA Fusion Association, Culham Science Centre, Abingdon, Oxfordshire, OX14 3DB, UK
[4] Japan Atomic Energy Agency, Naka, Japan
[5] Consorzio RFX, Association EURATOM-ENEA, I-35127 Padova, Italy

Received 31 December 2008, accepted for publication 13 February 2009
Published 10 March 2009
Online at stacks.iop.org/NF/49/045006

Abstract
The ITER neutral beam (NB) injectors are the first injectors that will have to operate under conditions and constraints similar to those that will be encountered in a fusion reactor. These injectors will have to operate in a hostile radiation environment and they will become highly radioactive due to the neutron flux from ITER. The injectors will use a single large ion source and accelerator that will produce 40 A 1 MeV D^- beams for pulse lengths of up to 3600 s.

Significant design changes have been made to the ITER heating NB (HNB) injector over the past 4 years. The main changes are:

1. Modifications to allow installation and maintenance of the beamline components with an overhead crane.
2. The beam source vessel shape has been changed and the beam source moved to allow more space for the connections between the 1 MV bushing and the beam source.
3. The RF driven negative ion source has replaced the filamented ion source as the reference design.
4. The ion source and extractor power supplies will be located in an air insulated high voltage (−1 MV) deck located outside the tokamak building instead of inside an SF_6 insulated HV deck located above the injector.
5. Introduction of an all metal absolute valve to prevent any tritium in the machine to escape into the NB cell during maintenance.

This paper describes the status of the design as of December 2008 including the above mentioned changes.

The very important power supply system of the neutral beam injectors is not described in any detail as that merits a paper beyond the competence of the present authors.

The R&D required to realize the injectors described in this paper must be carried out on a dedicated neutral beam test facility, which is not described here.

PACS numbers: 28.52.Cx, 41.75.Cn, 52.50.Gj

1. Background

Initially ITER will use two heating neutral beams that are designed to inject 33 MW of either 1 MeV D^0 or 870 keV H^0 into the ITER plasma. A third heating beam may be added later, bringing the total D^0 power that may be injected into ITER up to 50 MW. The injectors can produce either D^0 or H^0 beams, but in the following text D operation is assumed unless H operation is specifically indicated.

The beam power deposition in the plasma depends principally on the beam energy and the plasma density and it is necessary to deposit the beam power inside the so-called H-mode barrier, which is located between $0.9 < r/a < 1$, where r is the distance from the plasma centre and a is the minor radius of the plasma. For the ITER plasma this means that the D^0 energy has to be >200 keV. However, it is calculated that using low energy beams means that for the required input power (up to 50 MW), the particle flux would push the $D^+ : T^+$ ratio in the plasma away from the optimum of 1 : 1 and energies >300 keV are needed to avoid diminishing significantly the fusion reaction rate [1]. At such energies the production of neutral beams by the neutralization of accelerated positive ions becomes very inefficient and the neutralization of accelerated negative ions, D^-, has to be used. The neutralization efficiency

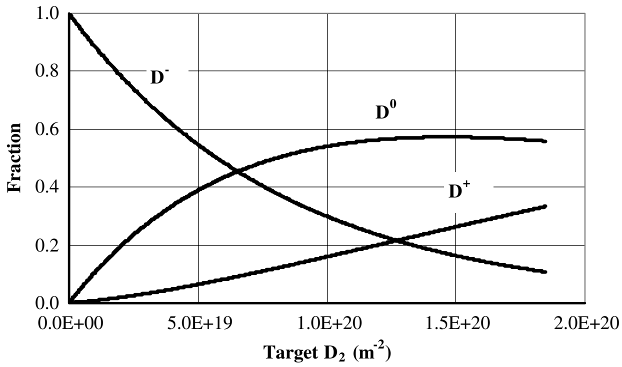

Figure 1. Beam species as a function of the gas target for a 1 MeV D^- beam passing through a D_2 gas target calculated using cross sections taken from [2].

is shown as a function of the beam energy in figure 1, with the neutralization being calculated with cross sections given in [2].

The HNBs will also drive current in ITER. For efficient NB current drive, both a high tangency radius, i.e. $R_{tan} > R_0$, where R_{tan} is the tangency radius and R_0 is the plasma major radius), and a high beam energy, $E \geqslant 1$ MeV, are required [1]. The tangency radius for the ITER HNBs is constrained by the port size, the need to pass between two of the ITER superconducting toroidal field coils and the need to have sufficient shielding around the injector duct to limit the neutron flux from ITER to the coils to acceptable values. The tangency radius is 5.28 m, which is significantly below the optimum for current drive. Nevertheless, the HNBs will drive currents of between 1.8 and 2.8 MA in ITER [3].

Compared to making D^+, making D^- is very difficult. Typically a D^- ion source consists of a box containing low pressure (<0.3 Pa) D_2 which is partially ionized (initial D_2 density $\approx 7.5 \times 10^{19}\,m^{-3}$, electron density $\approx 5 \times 10^{18}\,m^{-3}$) from which the D^- is extracted through a set of apertures in the plasma grid (PG), which forms one wall of the ion source and the first grid of the extractor. The D^- is created either by reactions within the plasma or by surface reactions involving the bombarding ions and atoms. In such an ion source there are many processes that lead to the destruction of D^-, which exacerbates the difficulties in producing high extracted current densities. Therefore to create a high power density beam, it is necessary to use high energies, not high current densities. The choice for ITER of 1 MeV is a compromise between the foreseen difficulties of developing higher energy, high power, power supplies and accelerators and the difficulty in making and accelerating high D^- currents.

2. The basic injector concept

As mentioned in section 1, the neutral beam is to be made by the neutralization of an accelerated D^- ion beam. The 1 MeV D^- beam is created by the beam source, which consists of an ion source directly attached to an extractor/accelerator. The ITER injectors are designed for an accelerated D^- current density of 200 A m^{-2} and an accelerated current of 40 A. The extraction of negative ions inevitably leads to the simultaneous extraction of electrons from the ion source. To avoid wastefully accelerating electrons to high energy, the extracted electrons are magnetically deflected onto the extraction grid, which is located 6 mm downstream of the PG at a potential of ≈10 kV with respect to that grid. The choice of an accelerated D^- current density of 200 A m^{-2} is governed by the state of the art of negative ion production and the power density of the co-extracted electrons that are dumped on the extraction grid.

The ion source is held at −1 MV and the D^- are accelerated up to ground potential. Unlike positive ion based systems the neutralizer is not closely coupled to the accelerator in order to minimize the average pressure in the accelerator. A gap between the accelerator and the neutralizer allows the gas entering the gap to be pumped away and the pressure at the accelerator exit kept low, <0.3 Pa. This keeps the loss of D^- by collisions with D_2 in the accelerator acceptable, ≈30% [4]. Nevertheless, many electrons are created inside the accelerator [5, 6], by a variety of processes. Those electrons are accelerated by the electric fields in the accelerator and most hit the accelerator grids or support structure, but a non-negligible fraction exits the accelerator; carrying a calculated power [5, 6] of ≈820 kW. Those electrons are deflected by a weak magnetic field onto a water cooled electron dump. The trajectories of the relatively massive 1 MeV D^- ions are almost unaffected by the weak magnetic field and they continue along the beamline into the neutralizer.

The neutralizer consists of a simple gas cell, open at each end, through which the beam passes. During the passage through the neutralizer, collisions of the D^- with the D_2 injected into the neutralizer leads to formation of D^0 by simple stripping of the outer electron from the D^-, and double stripping creates D^+. D^+ is also created by re-ionization of the D^0 produced from the D^-. With the optimum gas target the beam at the exit of the neutralizer consists of ≈60% D^0, ≈20% D^+ and ≈20% D^- (see figure 1).

After exiting the neutralizer the beam passes through the residual ion dump (RID) which consists of opposing pairs of electrically biased plates. The electric field deflects the charged components of the beam onto the plates, leaving the neutral beam to either impinge onto the calorimeter located just downstream of the ion dump or to continue into the duct leading to ITER. When intercepting the beam, the two panels making up the calorimeter form a V with the open end of the V facing the RID, with the axis of the V vertical. In this configuration the injector can be commissioned independently of ITER. When injecting into ITER, the V is opened so that the two panels are on either side of the beam. The measurement of the neutral power arriving on the calorimeter, together with the measurement of the downstream losses when the beam is injected into ITER, allows the neutral power to ITER to be determined.

Large cryopumps are placed each side of the beam path and the beamline components inside the injector to reduce the pressure downstream of the accelerator and downstream of the neutralizer exit to the required values. The pressure downstream of the accelerator must be low in order to minimize losses in the accelerator. The pressure downstream of the neutralizer must be low in order to minimize re-ionization of the D^0 by collision with the background D_2 as the D^+ thus formed would be deflected by the electrical field inside the RID or the stray magnetic field from ITER onto the RID panels, the open calorimeter, or the walls of the duct between the injector

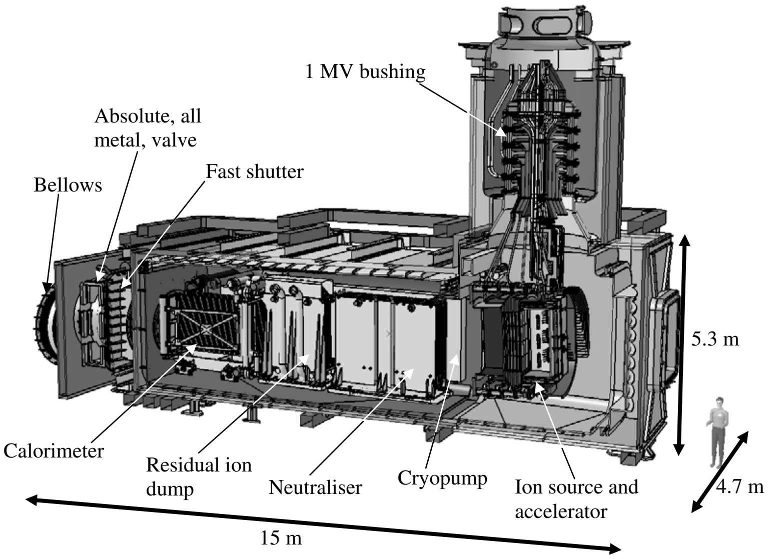

Figure 2. General cut-away view of an ITER heating neutral beam.

and ITER, thus reducing the power reaching the ITER plasma and unnecessarily heating the aforementioned components. A general cut-away view of an ITER heating neutral beam is shown as figure 2.

The electron dump, the neutralizer, the RID and the calorimeter are herein after referred to as the beamline components.

3. The injector vessels, shielding, and maintenance

The combination of the ion source, extractor and accelerator (see sections 5 and 6) is referred to as the beam source. The beam source is to be enclosed inside a beam source vessel (BSV) that is connected (welded) to the beamline vessel (BLV) which contains the beamline components and the cryopumps. Because of their size and weight, the two vessels will have to be manufactured and transported to ITER separately and welded together on site, inside the neutral beam cell. Changes to the building housing the tokamak and the injectors have made it possible to have an overhead crane installed in the neutral beam (NB) cell, the part of the building containing the injectors. To be able to use the crane to remove and install the beamline components and the cryopumps, for the initial installation and later maintenance operations, the BLV has been changed to have a rectangular cross section and a detachable lid and the cryopumps placed flat against the lateral walls of the BLV (see figure 2).

Neutrons from the tokamak will stream through the NB port and along the NB duct into the injector, activating the beamline components and the beam source. A massive iron shield, 150 mm thick, in combination with a set of 'active, correction, compensation, coils' (ACC coils) reduces the magnetic field inside the injector to acceptable performance. Without this magnetic field reduction system the accelerated D^- ions would be deflected from their ideal trajectory prior to neutralization. Since the neutralization of the ions is spatially distributed along the beam path, the effect of such magnetic deflection is to cause emittance growth and a global deflection of the neutral beam. The magnetic field reduction system consists of both the passive iron shield and the ACC coils, as this combination reduces the perturbation to the fields in the tokamak to a minimum. The passive magnetic shield also acts as a neutron shield, which prevents any significant activation of the NB cell.

4. The high voltage bushing

All the services to the beam source—water cooling, electrical power and D_2—enter the BSV via the high voltage (HV) bushing which is connected to the top of the BSV. The HV bushing is the interface between the vacuum in the BSV and the high voltage transmission line from the power supplies. The transmission line carries dc electrical power at various potentials down to −1 MV, and the RF power for the ion source. Insulation between the various conductors in the transmission line is provided by SF_6 at 0.6 MPa. The bushing itself is made up of five alumina cylinders of 1.46 m inner diameter, separated by stainless steel flanges. Outside each alumina cylinder is an epoxy cylinder and the interspace between the cylinders is filled with dry air at 1 MPa. This arrangement not only provides a double barrier for T_2 confinement but also it ensures a double barrier between the SF_6 and the injector vacuum, which is directly connected to the ITER vacuum vessel. This extra security is introduced since SF_6 is extremely damaging to the detritiation plant, which is connected to the torus. Figure 3 shows a cut-away of the upper two stages of the bushing.

A double flange closes the top of the bushing and all water and power at potentials between −990 kV and −1 MV pass through that flange. Water and power at −800, −600, −400, −200 and 0 kV passes through the intermediate flanges to the different stages of the MAMuG accelerator (see section 6). Water for cooling the accelerator grids and the ion source is introduced into the transmission line, from ground potential, via 'HV deck 2' (see section 9). An important parameter is the resistivity of the water, which determines the current flowing along the water from high voltage to ground. From a detailed

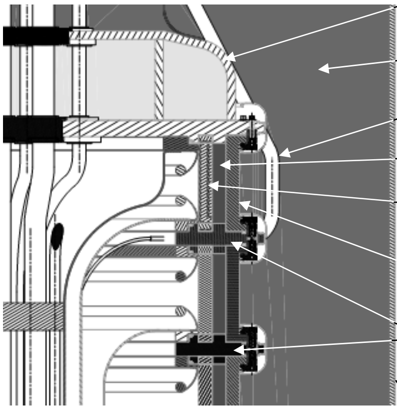

Figure 3. Computer model of cut-away of the upper two stages of the 1 MV bushing.

design study it has been concluded that the resistivity must be $>5\,\text{M}\Omega\,\text{cm}$. The power expected to each accelerator grid has been calculated using the EAMCC code, as shown in figure 4 [6]. The optimized design of the acceleration grid cooling leads to a temperature increase of $\approx 40\,^\circ\text{C}$ for each grid. Since the resistivity of water decreases as the temperature increases [7], it has been concluded that the water outlet temperature must be $<55\,^\circ\text{C}$. With the expected temperature rise in the grids ($40\,^\circ\text{C}$), the inlet temperature has to be $15\,^\circ\text{C}$.

The top of the BSV forms a frustum of a cone with the smaller end connected to the bushing. This allows the different high negative voltage connectors to be arranged such that the electric field between the conductors is minimized, and it allows space for connection and disconnection from the beam source.

5. The ITER neutral beam injector ion source

The only types of ion sources capable of meeting the extracted D^- current densities required for neutral beam injectors are the arc driven or radio frequency (RF) driven caesiated ion sources [8–10]. The RF driven ion source of the type being developed at IPP, Garching, Germany has been chosen for ITER because no filaments are used during the operation and hence there is no need to regularly replace filaments. This is an important consideration for ITER where the ion source will become activated during operation and all such operations must be carried out remotely. Most of the source development has been carried out on a 1/8 ITER size ion source. That source consists of a cylindrical alumina 'driver', ≈ 250 mm long, ≈ 220 mm inner diameter, around which is wound the RF coil, 5–6 turns, which is excited by RF power at a frequency of 1 MHz. Gas, H_2 or D_2, is injected into the driver and an inductively driven plasma is created. A Faraday screen (slotted orthogonally with respect to the RF coil) protects the alumina cylinder from bombardment by the plasma. The driver is connected to the 'expansion chamber', $\approx 600\times 220\times 330\,\text{mm}^3$, and the plasma from the driver is free to expand into that chamber. The wall of the expansion chamber opposite to the driver is the PG, the first grid of the extractor/accelerator. Negative ions are created by a variety of reactions in the plasma in the source, but, as with arc driven negative ion sources, the flux of negative ions to the PG is found to increase significantly if a small amount of caesium (Cs) is injected into the source. In caesiated sources the main D^- production mechanism is believed to be the backscattering of D, D^+, D_2^+ and D_3^+ from the metal surface of the ion source and the PG as D^-. Cs injected into the source forms a thin layer on the PG, which lowers the work function of the surface, which substantially increases the fraction of particles backscattered as D^-. In the caesiated sources the main D^- production is believed to be on the surface of the PG because the survival length of D^- in the source is only a few centimetres [11] and essentially only ions generated near or on the PG can reach the apertures in the grid and be extracted. Ions created on the PG surface enter the plasma of the ion source, and magnetic fields, electric fields and collisions (especially charge transfer collisions) influence their trajectories, and some return to the PG [11, 12]. The geometry of the PG surface can influence the initial trajectories of the D^- leaving the surface and there is experimental evidence that chamfering the annulus around the apertures can increase the D^- yield [9], and that geometry is now foreseen for the ITER ion sources (see figure 5).

During long pulse operation of the arc driven type of source it has been found that an unacceptably high flow of Cs into the source is needed to maintain the negative ion production rate necessary to ensure the required extracted D^- current density [13, 14]. The high flux of Cs into the filamented source arises from the need to maintain the optimum Cs coverage of the PG in the presence of tungsten evaporated from the filaments. The lack of filaments in the RF driven source may be the reason that there is a low consumption of caesium during operation of the RF driven source [16].

A critical aspect of ion source operation on ITER is the ability to operate stably for long pulses. This has been demonstrated for the filamented type source for 1000 s, but with reduced D^- current density because of tungsten contamination from the filaments [15]. The development of the long pulse operation of a small (1/8) and medium (1/2) size the RF source is ongoing. Stable operation for 800 s pulses has been demonstrated, although at H^- current densities less than required for ITER, but there is no deterioration in the performance compared with short pulse operation [16]. The work on long pulse operation is continuing with the aim to demonstrate 1 h operation with ITER relevant D^- current densities.

Maintenance of the RF driven source becomes necessary when the quantity of Cs in the source becomes excessive, either because of safety considerations (Cs is a very reactive element) or because the ion source performance deteriorates. Experiments are ongoing at IPP Garching to determine the required Cs injection rate during normal operation, and the maintenance frequency will be assessed once that is established. Based on the Cs consumption measured during long pulse operation of a 1/8 size RF driven source with 400 apertures in the PG [16], an initial assessment puts the consumption at $3.5\times 10^{-10}\,\text{g}\,\text{s}^{-1}\,\text{aperture}^{-1}$, which, if extrapolated to ITER gives $0.16\,\text{g}\,\text{h}^{-1}$ of operation. Thus if ITER operates for 100 days a year and has twenty 400 s pulses per day, with neutral beam injection throughout each pulse, a Cs reservoir of 40 g will suffice for one year of operation[6].

[6] Here it is assumed that the Cs consumption is due to loss through the

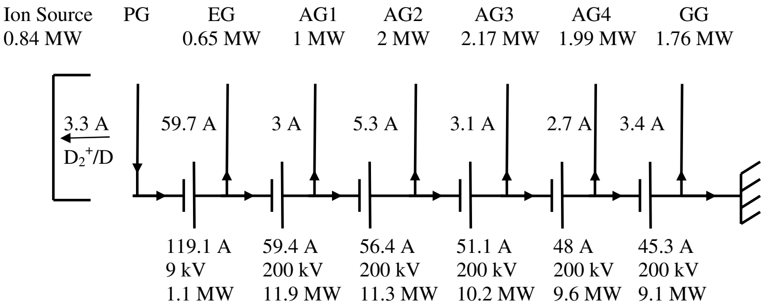

Exiting the accelerator:	Current	Power
Total (D^+, D^- & e)	42 A	42.7 MW
D^-	39.3 A	39.7 MW
Electrons	2.7 A	0.82 MW
D^+	0.07 A	0.02 MW
D^0		2.33 MW

Figure 4. Currents and powers for the ITER MAMuG accelerator with a 40 A D-beam with 15% halo exiting the accelerator. The calculations were performed with the EAMCC code. The source filling pressure was assumed to be 0.3 Pa and the gas density distribution was calculated with a Monte Carlo code. The labels below the figure give the power, voltages and currents in the extraction power supply and the five different stages of the acceleration power supply. (In this example the beam energy was actually 1.09 kV.)

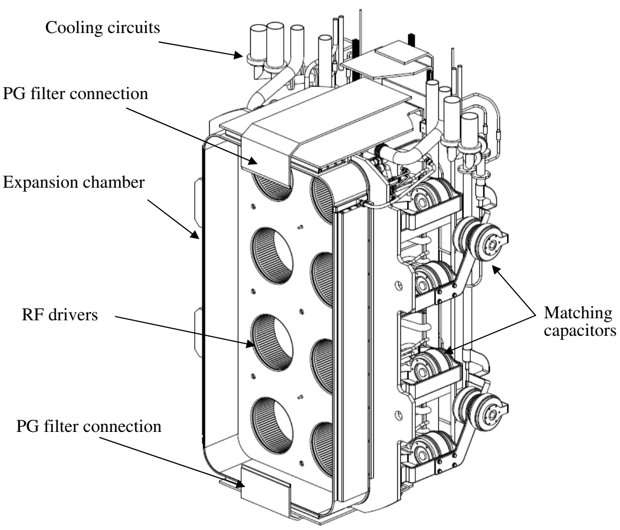

Figure 5. Drawing of the RF driven ion source. The outer diameter of the alumina cylinders of the drivers is 300 mm, and they are 172 mm long. The inner dimensions of the Faraday shield are diameter 275 mm, length 140 mm. The expansion chamber inner dimensions are $1.77 \times 0.87 \times 0.22\,\mathrm{m}^3$, height$\times$width $\times$ depth. The eight drivers operate in horizontal pairs and the power distribution between the pairs of drivers is adjustable. Fixed value matching capacitors in combination with frequency variation allow good matching of the load and the power system.

D^- ions are rather delicate, having an electron affinity of only 0.75 eV. This is an advantage in that they are easily neutralized after acceleration, but a disadvantage as they are also easily neutralized by collisions in the accelerator. The latter process is called stripping to distinguish it from the desired post acceleration neutralization. Therefore the pressure in the accelerator must be minimized, which leads to the requirement that the ion source, which is directly connected to the accelerator, must operate at low pressure. The highest acceptable source filling pressure (the pressure measured prior to plasma formation in the source) has been calculated to be 0.3 Pa. The RF driven source has achieved the extracted D^- and H^- current densities and co-extracted electron fractions required for the ITER system at the filling pressure of 0.3 Pa [8–10].

Stripping leads not only to the loss of D^- but also to electron generation, then acceleration in the pertaining electric field. Also electrons are generated inside the accelerator by a variety of processes such as direct ionization of the background gas by the accelerated D^- and secondary electron generation by particle impact on the grid surfaces. Electrons generated in the accelerator do not follow the same trajectories as the D^- ions and most are intercepted on the grids, consequently depositing power to the grids.

As mentioned above, the source required for the ITER injectors is $\approx$8 times larger than the sources used for the development. The planned extrapolation is modular, having eight drivers that are similar to those of the development sources, arranged in four pairs attached to a single large expansion chamber, as shown in figure 5. This arrangement allows the power to the different drivers to be varied in order to optimize the flux of negative ions to the apertures in the PG.

A new element in the design of the ion source is the recognition of the high power density at the rear of the source that will arise from backstreaming positive ions. Positive ions can be created in the accelerator by several processes, the most important being the direct ionization of the background D_2 by accelerated D^-. The recently developed EAMCC code is capable of calculating the positive ion production in the accelerator and following them as they are accelerated back onto the grids or into the ion source. For the ITER ion source with the MAMuG accelerator the total backstreaming ion power is calculated to be 0.84 MW, with a power density of $>50\,\mathrm{MW\,m^{-2}}$ in small (<2 mm diameter) spots on the metal surfaces of the rear of the drivers [5, 6], and a sophisticated cooling system has been developed to cope with those powers and power densities.

apertures in the accelerator. It is possible that other mechanisms, such as oxidation, are the actual reason fresh Cs has to be introduced into the source.

6. The ITER neutral beam injector extractor and accelerator

Two 40 A, 1 MeV, D^- accelerator concepts were developed for ITER NB injection: SINGAP [17] and MAMuG, the former being developed by CEA Cadarache, France, the latter by JAEA, Naka, Japan. Where SINGAP accelerates the pre-accelerated (40–200 keV) beams in one single step to 1 MeV, MAMuG does this in five stages. Recently a version of the SINGAP accelerator has been tested on the MeV test facility at Naka, where the MAMuG concept has been developed. This allowed a direct comparison between the performance of the two accelerators on the same test facility with the same power system and diagnostics. The experiments confirmed that the voltage holding of the SINGAP accelerator is worse than that of the MAMuG one (by ≈200 kV), and that the power carried by electrons that exit the accelerator from SINGAP is much higher than from MAMuG [18, 19].

The reason that the voltage holding is lower for SINGAP than MAMuG has not been unequivocally identified. It might be explained by some default in the electrostatic configuration used for the Naka experiments with SINGAP, which was significantly different from that with the MAMuG accelerator and different from that which would prevail in an ITER injector with either a SINGAP or a MAMuG accelerator. It might also be explained by clump theory [20], which would predict a voltage holding limit of ≈600 kV [19], in reasonable agreement with the experiments. (The same breakdown voltage law predicts that the short gaps in the MAMuG accelerator should easily withstand the required 200 kV.) However, it should be noted that it has been observed that although clump theory shows reasonable agreement in gross details with experiments, there are significant discrepancies in detail [19, 20].

Electrons are created in the accelerator by a variety of processes in addition to the direct extraction from the ion source. This has been studied in detail with the EAMCC code for both accelerator concepts [5, 6]. EAMCC can calculate the power, particle flux, power density and emittance of the exiting electrons. The power in the exiting electrons from an ITER size SINGAP accelerator is calculated to be 8 MW compared with 0.82 MW from an ITER size MAMuG accelerator. Whilst it is possible to collect such powers on a water cooled electron dump, there would be substantial electron reflection (≈30% in power) from the dump and it would be extremely difficult to shield the cryopumps from that power whilst maintaining the required pumping speed in the accelerator to neutralizer gap.

The design of the electrostatic acceleration system is quite complex and only a brief description is given here. With a MAMuG accelerator the ions are extracted and then accelerated through a series of aligned apertures in grids at increasing positive potentials. The ITER extractor/accelerator consists of the PG, an extraction grid and five acceleration grids, each at ≈ + 200 kV with respect to its predecessor. Each grid is mounted on its support structure, its 'grid holder', which is itself supported from the grid holder of the next downstream grid holder and so on. The support of each grid holders (apart from the grounded grid) consists of a set of alumina 'post insulators' distributed around the grid holder. Such a support structure is quite transparent for gas flow. This allows gas to flow laterally from the gaps between grids, then around the beam source to the cryopumps Calculations have shown that it is important to maintain as high a lateral transparency (for gas) as possible in order to minimize stripping losses [4]. Figure 6 shows a model of the extractor/accelerator attached to the RF driven ion source.

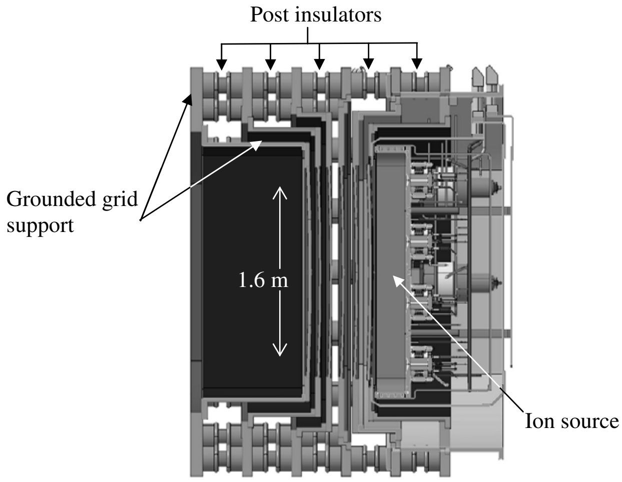

Figure 6. Computer model of the ITER beam source.

The grounded grid holder is attached to the BSV (see section 3) at the top via a hinge that allows rotation of the beam source in the vertical plane and at the bottom by a support that can be moved axially from outside the vacuum envelope. This allows the beam source to be tilted by ±9 mrad so that the beam is deposited either close to the axis of the plasma in ITER, or 'off-axis', as required by the tokamak physicists. The main considerations in the design are:

- It is assumed that the ions are emitted normal to a curved surface that is defined according to the Child–Langmuir law and is limited by the edges of the aperture in the PG. The ions are then initially convergent, but space charge forces change the degree of convergence, and would lead eventually to the beamlet[7] becoming divergent. However, after a few millimetres the ions pass through the extraction grid. Then into the first acceleration gap. As the field in the extraction gap is stronger than that in the acceleration gap, the apertures in the extraction grid form a negative electrostatic lens. The voltages have to be such that the beamlet leaving the extraction grid is sufficiently convergent to resist the space charge expansion that will occur as the beamlet passes through the first acceleration gap. The acceleration gaps are made progressively shorter so that the apertures in all the subsequent acceleration grids but the last form slightly convergent lenses to counteract the space charge expansion in the following gap. The apertures in the last grid, the grounded grid (GG), always form negative lenses, so the apertures in the preceding grid have to produce sufficiently convergent beamlets that when they exit the accelerator they are (nominally) parallel. It is assumed that space charge neutralization occurs close to the exit of the GG due to

[7] The name 'beamlet' is given to the beam of ions from a single aperture, and the name 'beam' to the sum of all the beamlets.

Table 1. Main parameters of the ITER 1 MV MAMuG grids.

	PG[a]	EXG[a]	A1G[a]	A2G[a]	A3G[a]	A4G[a]	GG[a]
Potential (kV)	−1000	−990	−800	−600	−400	−200	0
Minimum aperture diameter (mm)	14[b]	11[b]	16[c]	16[c]	16[c]	16[c]	16[c]
Thickness (mm)	9	17[d]	20[e]	20[e]	20[e]	20[e]	20[e]
Gap from preceding grid (mm)		6[f]	86	77	68	59	50

[a] PG—plasma grid, EXG—extraction grid, AG*—acceleration grid *, GG—grounded grid, which is the last acceleration grid.
[b] The diameter is not constant. The minimum diameter is indicated. An increase in aperture diameter to 14 mm is being considered.
[c] Constant aperture diameter (the hole is cylindrical).
[d] A decrease in thickness is being examined.
[e] A reduction in the thickness of the acceleration grids to 10 mm is being studied.
[f] A reduction in extraction gap to 5 mm is being considered.

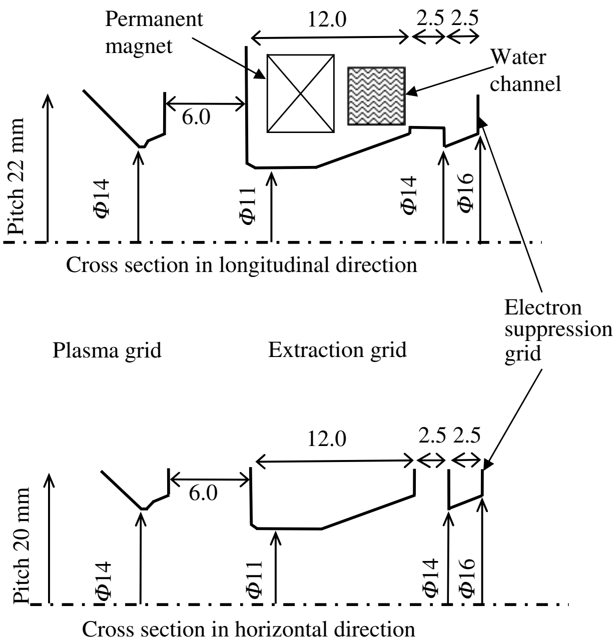

Figure 7. Geometry of the MAMuG plasma grid (PG) and extraction grid (EG), dimensions in millimetres. The extraction grid incorporates a structure called 'Electron Suppression Grid'. Its purpose is not only to suppress electrons but also to correct, by offsetting its aperture, for the magnetic steering induced by the $5.6 \times 4.9\,\mathrm{mm}^2$ permanent SmCo magnet ($B_{\mathrm{surface}} = 0.96$ T). The water cooling channel has a square cross section of $4 \times 4\,\mathrm{mm}^2$. The shape of PG upstream (to the left) of the knife edge is chamfered at 45° as this appears to enhance the negative ion yield.

ionization of the background gas by the beamlets. The basic parameters of the grid spacing and the apertures are as in table 1. The precise geometry of the PG and EG is shown in figure 7.

The current design of the injectors assumes that the beamlet can be characterized by a 'core' divergence of $\leqslant$7 mrad carrying 85% of the power with the other 15% having a significantly higher divergence (15–30 mrad). The beamlet core divergence from the MAMuG and SINGAP prototype accelerators has been measured to be $\approx$5.5 mrad [19].

- In order to have a 40 A D^- beam 1280 apertures are needed, giving a total area for the apertures in the PG of $0.2\,\mathrm{m}^2$ ($0.2\,\mathrm{m}^2 * 200\,\mathrm{A\,m}^{-2} = 40$ A). (The accelerated current density is taken as the accelerated current divided by the PG aperture array area as at the apertures in the other grids the beamlet size is not equal to the aperture size.) The aperture array is organized to produce four 'column' beams that pass through the four channels of the neutralizer and RID (see section 7.3). Additionally the grid at each potential is divided into four 'segments' vertically for ease of assembly and thermal expansion reasons. The result is 16 groups of 5×16 apertures as shown in figure 8(*a*).
- Each grid has to be actively cooled and the extraction grid has to incorporate the electron suppression magnets. The position and size of the electron suppression magnets and the shape of the apertures in the extraction grid have to be carefully designed to ensure that few electrons escape into the acceleration region.
- Accelerating to high energy the electrons that are co-extracted from the ion source along with the negative serves no useful purpose; it would simply waste power and melt downstream components. Therefore, the co-extracted electrons are dumped onto the extraction grid by a magnetic field created partially by the magnetic filter of the ion source and partly by permanent magnets embedded in the extraction grid (the 'electron suppression magnets'). The electron suppression magnets are oriented so as to create a vertical field that is orthogonal to the beam direction and the field from the filter of the ion source. Having the source filter and suppression magnet fields orthogonal gives the minimum leakage of the extracted electrons through the extraction grid and into the accelerator. The field has only a small effect on the ion trajectories, but this has to be corrected to maximize the transmission to ITER. The combination of the PG and the extraction grid (EXG) is known as the extractor.
- To maximise the transmission to ITER each group of apertures is aimed at the centre of the aperture in the ITER blanket (when the beam is not tilted—see above), 25.48 m from the grounded grid. This distance is 2 m longer than the design of 2001 [23] due to the introduction of an all metal gate valve, 1.7 m overall length, and a move backwards of the beam source by 0.3 m to ease access to the connections between the 1 MV bushing and the beam source. The beam group aiming will be achieved by machining the grid support structure such that each segment is inclined in the vertical plane by the required amount, and by machining the grid segments to have each

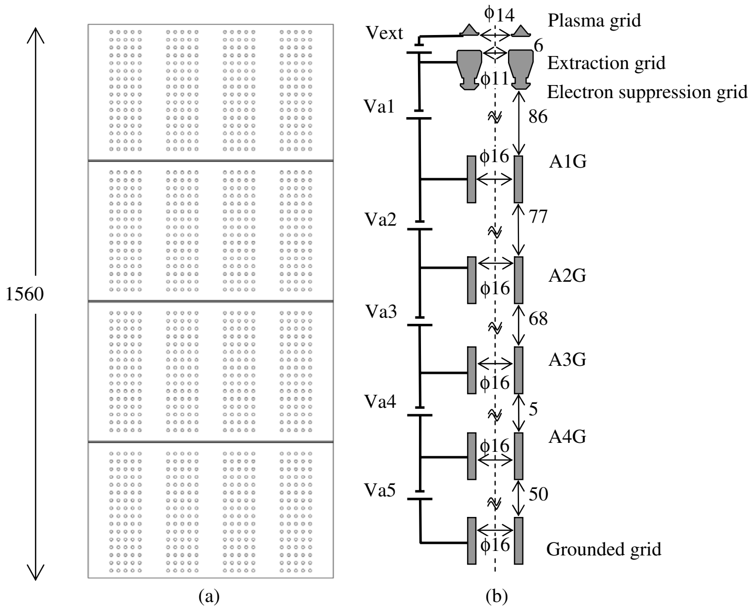

Figure 8. Aperture array on the PG. (*a*) Shows the front view of the whole array. (*b*) Shows a single 'beamlet' channel along the accelerator axially. The scales are not the same. All dimensions are in millimetres.

group of apertures inclined in the horizontal plane by the required amount. In addition all the beamlets in one group must be aimed in the horizontal plane at the centre of the appropriate exit of the RID, which is the narrowest aperture (in the horizontal direction) in the beamline. The RID exits are 7.2 m from the grounded grid. The beamlets have a finite divergence and it is found that aiming them at the vertical centreline of the RID exits maximizes the transmission of the beamlets to the torus. This aiming will be achieved by using an offset aperture steering on the grounded grid. Further steering in the vertical plane could improve the transmission, but this is not possible by the offset aperture steering as the beamlets are then too close to the aperture walls, which can give rise to aberrations and interception on the grids. Figure 9 shows schematically the beamlet aiming of the ITER beam source.

- In addition to steering the beamlets, it is necessary to counteract the effect of the field from the electron suppression magnets in the extraction grids on the ion trajectories and of beamlet—beamlet repulsion at the edges of each group of beamlets. This will be achieved by the offset aperture steering at the exit of the extraction grid (labelled the 'electron suppression grid' in figure 7) and by making the downstream surface of the grid around each group of apertures higher than the surface of the apertures themselves, which creates a curvature in the local electric field that pushes the outer beamlets inwards. The detailed design of this is ongoing using a combination of 2D theory and 3D numerical computation.

ITER will begin operation with H^+ or He^{++} plasmas as this allows ITER and all the sub-systems to be commissioned without becoming radioactive. During this phase it is required to inject H^0 beams, not D^0 beams. This is technically feasible, within the limitations of the system. Operation with H^- with good beam optics (as required to avoid excessive loads to the beamline components and good beam transmission)

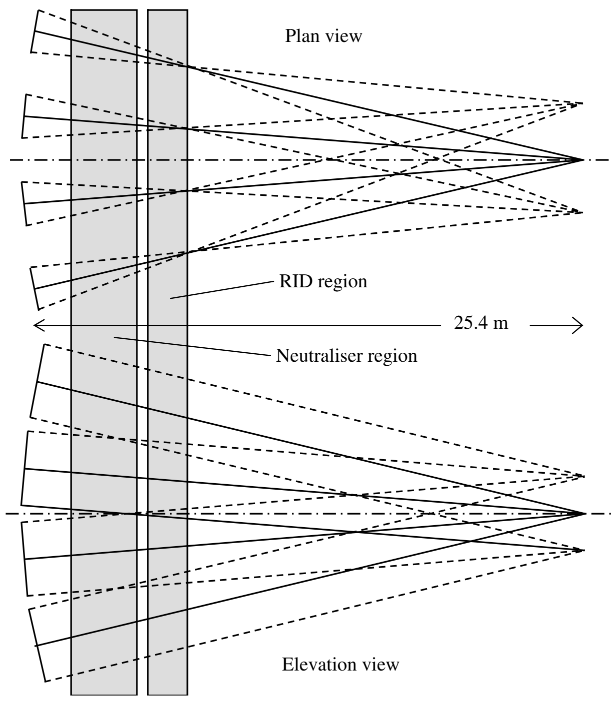

Figure 9. Schematic of the beamlet steering of the ITER beam source. The scales in the vertical and horizontal directions are not the same and for clarity only the centrelines of the edge beamlets and of the beam groups are shown. The upper half of the figure shows the steering in the horizontal plane where each beam group is aimed at the NB duct exit, but the axes of the beamlets coincide at the exit of the RID, 7.2 m form the grounded grid. The lower half of the figure shows the steering in the vertical plane. All the beamlets from one group are parallel, but each group is aimed at the centre of the aperture in the ITER blanket when the beam is not tilted.

means operating at the optimum perveance of the accelerator, which is an inverse function of the square root of the mass of the accelerated ion. Practically that means that a full power (40 MW) H^- beam will be obtained when the acceleration voltage is 870 kV and the accelerated beam current is 46 A.

7. The beamline components

The beamline components are the components located downstream of the accelerator, within the neutral beam vacuum vessels. Each component is designed to be able to cope with the expected power with assumed beam and beamlet characteristics.

Should the beamlet optics turn out to be better than expected (see section 6), the neutral beam power that would be transmitted to ITER would exceed the nominal 16.5 MW. However that could lead to power densities on the calorimeter and/or the RID that exceeds the design values. In that case the beam source can be operated at lower power (reduced beam energy) to the point that the power to ITER is 16.5 MW, in order to reduce the power to the critically loaded component.

7.1. The electron dump

As mentioned in section 2, it is calculated that ≈0.8 MW of electrons will exit the MAMuG accelerator along with the D^- beam. Those electrons will be deflected onto the front of the neutralizer, the neutralizer floor and, if necessary, a water cooled electron dump. It is possible that the far field from the magnetic filter of the ion source will be sufficient to deflect the electrons, but if necessary columns of magnets will be placed each side of the column beams emerging from the accelerator will be introduced to produce an optimal deflection of the electrons. A study of the power footprint of electron beam, the need for additional deflection and the design of the electron dump has just started, so the design cannot be described here. Although preliminary studies have shown that the dumped electron power can be readily handled, it is worth mentioning that a more serious difficulty arises in the control of the electron power reflected from the surfaces on which the electrons impinge. Up to 30% of the incident power could be reflected [2] and it must be assured that less than ≈10 kW reaches the 80 K surfaces of the cryopumps, and that less than ≈100 W hits the 6.5 K surfaces in order to maintain controlled operation of the cryopump. That will be achieved using suitably placed baffles. The baffles must have as high a gas transparency as possible in order not to reduce the pumping speed in the region between the accelerator and the neutralizer. Any reduction in pumping speed in that region leads to increased losses in the accelerator by stripping, increased power to the accelerator grids and less accelerated ions.

7.2. The neutralizer

A simple D_2 gas neutralizer has been chosen as there are little or no advantages to other gases and alternatives such as a lithium [24], plasma [25] or photon [26] neutralizer require significant development. With a negative ion accelerator the mean pressure in the accelerator has to be minimized to keep the losses due to stripping in the accelerator to an acceptable level. Therefore, the neutralizer must be decoupled from the accelerator, creating a pumped region between it and the accelerator. The neutralizer entrance is located 1.9 m downstream of the grounded grid.

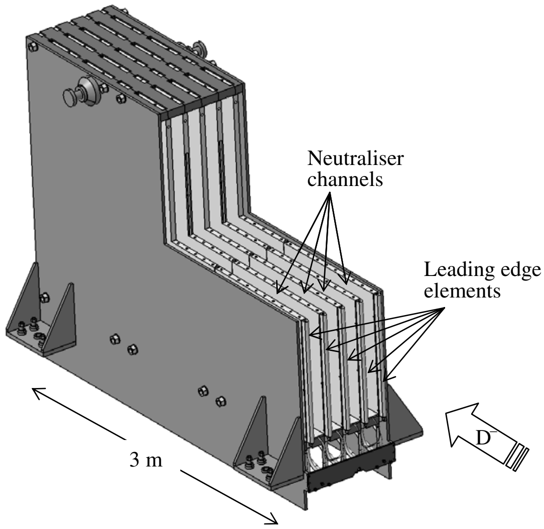

Figure 10. A cut-away CAD model of the neutralizer partially cut-away to show the four channels. The leading edge elements protect the front of the channel walls from direct interception of be beam.

To create the required gas target, gas is admitted 2 m along the neutralizer. To reduce the required gas flow, the neutralizer is subdivided to have four rectangular cross section channels side by side, along which pass the four column beams from the accelerator—see figure 10. This subdivision decreases the total gas conductance of the neutralizer, hence the required gas flow, by approximately a factor 2 compared with a single channel neutralizer. Each channel is 3 m long, 1.7 m high, 105 mm wide at the entrance, and 95 mm wide at the exit. The finite divergence of the beamlets from the accelerator and probable small errors in alignment of the beam or the neutralizer mean that some power is directly intercepted on the neutralizer walls. Each channel is made up of two copper walls (the inner walls of the neutralizer consist of two walls), and each copper wall is made of three sections, each 1.82 m high and 1 m long axially. The power density is low and the copper walls are cooled by serpentine channels with a pitch in the axial direction of 71 mm. The 18 mm internal diameter cooling channels are created by deep drilling the 44.1 mm thick walls with e-beam welded plugs as needed. Special elements protect the leading edges of each neutralizer wall against direct beam interception. These are swirl tubes with a cross section shaped axially so that the incident power is evenly spread over the element axially, being narrower at the side facing the accelerator and slightly wider than the neutralizer wall at the entrance to each neutralizer channel.

Gas is to be introduced into the neutralizer ≈2 m from the entrance. Although introducing the gas midway along the neutralizer would minimize the gas flow required to have the required neutralization target, introducing it at 2 m from the entrance does not significantly increase the flow, but it reduces the flow towards the neutralizer entrance, thus reducing the pressure at the exit of the accelerator and the stripping losses in the accelerator. Although the flow towards the neutralizer exit increases compared with introducing the gas at the neutralizer midpoint, which increases the pressure downstream of the neutralizer, and hence the re-ionization losses, the overall losses are reduced.

The two most important reactions occurring in the neutralizer are

$$D^- + D_2 \Rightarrow D^0 + D_2 + e$$

and

$$D^0 + D_2 \Rightarrow D^+ + D_2 + e.$$

Because the latter leads to the loss of the D^0 created by the neutralization of the D^-, there is an optimum target at which the fraction of D^0 in the beam passes through a maximum. At the optimum target ($\approx 1.4 \times 10^{20}\ m^{-2}$), the beam consists of $\approx$60% D^0, and $\approx$20% each of D^+ and D^-, see figure 1.

Heating of the gas in a simple gas neutralizer by high power positive ion based neutral beams is a well established phenomenon that reduces the gas density because of the increased conductance out of the neutralizer [27–31]. The gas in the neutralizer is heated by processes involving the plasma created by the beam [27] such as molecular dissociation and the acceleration of plasma ions across the sheath at the neutralizer wall and their reflection as energetic neutrals. The resulting reduction in neutralization cannot be easily redressed by increasing the gas flow into the neutralizer to increase the gas target since the beam heating increases with increased gas density, and it is found that the rate of increase in the neutralization target with gas flow is extremely slow.

A model of this phenomenon was developed for, and benchmarked against, results obtained with, the JET positive ion system. This model has been adapted and applied to ITER relevant negative ion beams and neutralizer [32]. The model predicts that the gas heating on the ITER heating beam system will be moderate, with gas temperatures less than 120 K above that of the neutralizer wall, which would result in a reduction of 6% in the neutralization efficiency.

7.3. The residual ion dump

The charged fractions of the beam are deflected out of the beam path by the RID leaving the neutral beam to either continue and be stopped at the downstream calorimeter (see section 7.4), or continue to the tokamak. The RID consists of five vertical panels forming four channels in line with the channels of the neutralizer.

The 1st, 3rd and 5th panels (counting from one side) are held at 0 kV whilst 2nd and 4th panels are biased by ≈ -20 kV to deflect the charged particles onto the water cooled panels (up to 25 kV is available from the power supply), which are made up of an array of vertical, rectangular cross section, swirl tubes. Each of the inner panels receives equal power on each side, but the two outer panels receive power from one side only. This design is compact, yet it spreads the power in the charged beams (up to $\approx$17 MW) over eight surfaces. The disadvantages are that there will be some secondary electrons generated at the surfaces by the positive ions that will be accelerated by the applied 20 kV to the opposing panel and that the gas generated by the dumped beam has to be pumped away through the narrow channels. Figure 11 shows a cut-away CAD model of the RID.

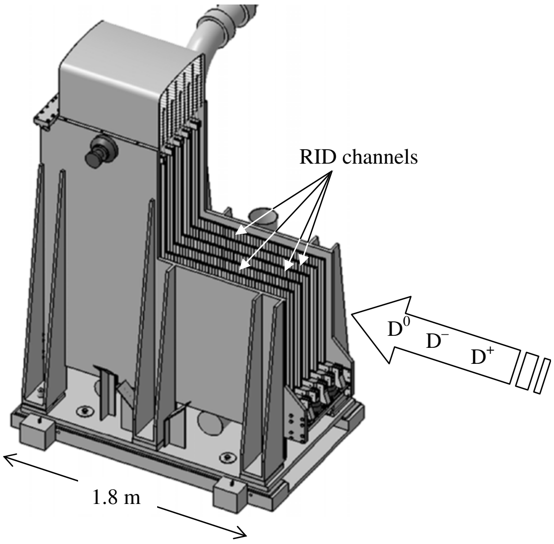

Figure 11. A cut-away CAD model of the RID showing the four channels along which the four 'column' beams pass.

As mentioned at the beginning of this section, the beamlet optics might turn out to be better than expected. That could lead to power densities on the RID that exceeds the design values. Two strategies are available to avoid this:

(a) The beam source can be operated at lower power (reduced beam energy) to the point that the power to ITER is 16.5 MW, reducing the power to the RID.
(b) The ion beams can be swept back and forwards over the surfaces of the RID by adding an alternating component, either trapezoidal or sinusoidal, to the voltage applied to the biased plates, thus reducing the average peak power density to the RID surfaces. The alternating voltage can be adjusted up to $\pm$5 kV.

The entrance to the RID is located 500 mm downstream of the neutralizer (5.4 m from the grounded grid) to allow adequate pumping of the region between the neutralizer and the RID. Each panel, is made up of an array of interlocked vertical rectangular cross section swirl tubes, with an active cooling height of >1.7 m. Each panel is 1.8 m long in the axial direction, 106.1 mm wide at the entrance and 94.8 mm wide at the exit. The width of the panels is 20 mm and the leading edges are in the shadow of the neutralizer exit and they are therefore protected from any direct interception of the beam.

Recent calculations have confirmed that this design will not lead to plasma formation in the channels (via beam ionization of the residual gas) which could null the applied deflection field [33].

7.4. The beamline calorimeter

The beamline calorimeter consists of two panels, which, in the intercepting mode, form a V with the apex of the V being vertical, the open end of which faces the RID, with an axial length of 2.6 m. The open end is 531 mm wide, wider than the beam emerging from the RID, so that the entire emerging beam impinges on the calorimeter. The panels can be rotated so that when fully 'open' they are at either side of the beam, and the beam passes into the NB duct and thence to ITER.

The panels are made up of a horizontal array of circular cross section swirl tubes, ≈2.5 m long. The measurement of the inlet and exit temperature of each tube allows the vertical profile of the beam to be quite accurately determined, albeit integrated over an axial distance of ≈2.5 m.

The main purpose of the calorimeter is to allow the injector to be commissioned independently of ITER. Combined with measurements of the losses in the NB duct, it also allows the injected power to be determined.

7.5. *BLV exit scraper*

A variety of high energy particles may hit the end wall of the BLV, which is made of stainless steel and is not cooled. Although the power and the power density expected on to the end wall of the BLV are low, the long pulses foreseen on ITER mean that the total energy deposited locally can be significant and a cooled protection structure is necessary. High energy particles that will hit the end wall include some of the re-ionized D^0 created in the RID, reflected D^0 and some reflected D^+ from the RID panels, and ions created by re-ionization of beam particles after the RID that are deflected by the residual magnetic field in the injector.

A scraper at the BLV exit is needed to ensure that no direct interception of beam particles occurs on the NB bellows screen (see section 8.3).

Thus the end wall of the BLV around the exit aperture is to be protected from any power deposition by a cooled structure around the exit which extends through the exit aperture and acts as a beam scraper.

7.6. *Cryopumps, gas flow and beamline component positions*

The gas flow into the injector and the cryopump configuration are extremely important factors in the design of a negative ion based neutral beam injector. The relative positions of the beamline components are also very important as there must be sufficient distance between the accelerator and the neutralizer and between the neutralizer and the RID to allow effective pumping of those regions. Consequently in the ITER beamline the gap between the exit of the support of the last acceleration grid (the grounded grid) and between the neutralizer and RID are set to 1.9 m and 0.5 m, respectively.

- The gas flow into the ion source determines largely the pressure in the accelerator, hence the stripping losses and the power to the acceleration grids.
- The distance between the accelerator and the neutralizer determines the access for pumping gas emerging from the neutralizer and that from the ion source and accelerator, hence the pressure in that region, which influences the stripping losses in the accelerator.
- The distance between the neutralizer and the RID determines the access for pumping gas emerging from the neutralizer exit and the RID, hence the pressure and the re-ionization loss in that region and downstream the RID.
- The pumping speed of the cryopump and its geometry and position in the beam line are major factors in determining the effective pumping speed at any point along the beamline.

The gas pressure in the BLV is such that molecular flow conditions exist and the gas density distributions due to the flow from the ion source and neutralizer can be calculated independently and then added to get the distribution with both gas flows present. The optimum gas target for the neutralization of the 1 MeV D^- beam is $1.4 \times 10^{19}\,m^2$ and is reached with a source filling pressure of 0.3 Pa. For the neutralization of the 870 keV H^- beam the filling pressure in the neutralizer must be increased to 0.45 Pa to get the optimum gas target of $2.2 \times 10^{19}\,m^{-2}$. For the gas profile calculations in the BLV two cryopumps with a pumping area of 2.3 m × 8m (height × length) have been used. The pumps are located each side of the beamline components, against the vessel walls. The cryopumping system of one injector achieves a total pumping speed of $3.6 \times 10^3\,m^3\,s^{-1}$ for D_2 and $4700\,m^3\,s^{-1}$ for H_2.

It is necessary to inject H^0 during the H–He phase of ITER operations as D^0 would lead to a significant D^+ density in ITER, and D–D reactions would then lead to some unwanted activation of the machine during that operation phase. This means that the cryopumps will have to be capable of pumping H_2 at the desired pressure (≈2×10^{-4} Pa at the exit of the BLV). Using condensation pumps this would require pumping surfaces at ≈3.8 K, in order to reduce the vapour pressure of the condensed H_2 to a sufficiently low value that the pumping is effective. For the very large cryopumping system this results in a strong demand on the cryogenic supply.

The use of cryosorption pumps based on activated charcoal on stainless steel plates means that the surface temperatures for pumping hydrogen can reach 10 to 15 K without losing pumping efficiency. The cryosorption pumps are cooled by supercritical helium at an inlet temperature of 4.7 K at 0.4 MPa absolute pressure and a predicted outlet temperature of ≈6.7 K. The cryopumps consists of two 'panels' situated either side of the beamline components in the BLV, close to the walls. The active (pumping) surface of each is 8 m in length, starting at the axial position od the neutralizer entrance, and 2.3 m in height.

Detailed calculations of the gas profiles along the entire beam line have led to the conclusion that:

- With a source filling pressure of 0.3 Pa the gas flow from the ion source will be $3.6\,Pa\,m^3\,s^{-1}$ in D_2 operation and $5.1\,Pa\,m^3\,s^{-1}$ in H_2 operation.
- In the neutralizer the gas should be introduced into the neutralizer channels at 2.0 m from the neutralizer entrance as that reduces the pressure between the accelerator and neutralizer without seriously increasing the total flow into the neutralizer.
- The pressure in the neutralizer at the gas introduction point to get the optimum target for neutralizing 1 MeV D^- is 0.3 Pa and leads to a gas flow out of the neutralizer of $19\,Pa\,m^3\,s^{-1}$.
- The pressure in the neutralizer at the gas introduction point to get the optimum target for neutralizing 870 keV H^- is 0.47 Pa and leads to a gas flow out of the neutralizer of $43\,Pa\,m^3\,s^{-1}$.
- The pressure between the accelerator and the neutralizer should be less than ≈0.025 Pa.
- An acceptable gas density distribution in the BLV can be achieved with cryopumps located each side of the beamline components, against the walls of the BLV, which start at the entrance of the neutralizer and extend

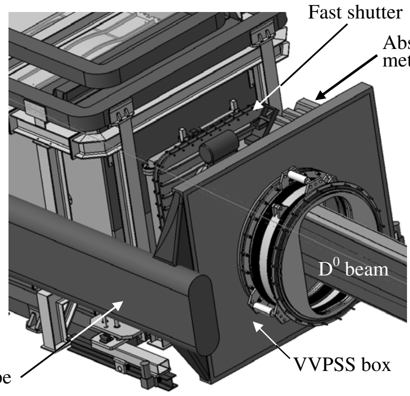

Figure 12. CAD model showing the exit of the BSV and the VVPSS box.

downstream for ≈8 m if the effective capture coefficient (at the 80 K thermal screen surface) for D_2 is ≈0.3. A practical design of cryopumps with that characteristic has been developed [34, 35].

8. The NB duct and the downstream components

A 'fast shutter' is connected to the exit of the BSV, followed by a gate valve, the vacuum vessel pressure suppression system connection box (the 'VVPSS box'), the 'NB drift duct', and the 'NB duct', see figures 2 and 12. Because the surfaces of all these components will be directly exposed to the tokamak vacuum with no intervening cryopumps, they will, like all surfaces facing the tokamak vacuum, have to be baked to 150 °C.

8.1. The fast shutter

The fast shutter is basically a light metal sliding 'door' that, when closed, shuts off the NB injector from the downstream NB components and duct and the tokamak. It is designed so that in the closed position the gas conductance is low ($<10^{-4}$ m^3 s^{-1} with molecular flow conditions applying). The fast shutter will normally be closed when there is no beam injection. It serves two purposes: firstly it allows the periodic regeneration of the injector cryopumps with insignificant gas flow to the tokamak. Secondly it prevents the ingress of gases (including T_2) into the injector from the tokamak during normal operation, except when injection is taking place. This is important when the tokamak is starting, when it is filled with gas to >0.01 Pa with D_2/T_2), and at the end of the pulse when all the gas leaves the tokamak, either via a controlled shutdown or by a disruption. The shutter is 'fast' in that it will open/close in <1 s, which is short compared with the vacuum time constant of the NB duct and the tokamak.

The detailed design of the shutter is not yet complete, but a 1/4 scale prototype was built and successfully tested for >5000 opening closing cycles. The mechanism used magnetic coupling between a 'master system' at atmospheric pressure and a 'slave system' in vacuum to produce the required movement of the shutter, thus avoiding the use of bellows. No baking system was incorporated in the prototype.

In order to be able to close rapidly the shutter door must have a low mass, and therefore it is not expected to be capable of withstanding a significant pressure differential, e.g. ⩾0.1 MPa, such as is expected if there is a large loss of coolant event inside the tokamak. Hence during such an event, unless the gate valve (see section 8.2) is closed, steam; activated dust, D_2, and T_2 will enter the injectors. However, such events are expected to be rare and the subsequent repair and clean-up of the tokamak will be very long. The strategy for the injectors clean-up following such an off-normal event has yet to be developed.

8.2. The absolute valve

A gate valve, usually called the 'absolute' valve at ITER, has been introduced between the exit of the fast shutter and the duct to the tokamak, which allows maintenance of the injector with the tokamak under vacuum, or maintenance of the tokamak with the injector under vacuum. As the fast shutter cannot withstand a large pressure differential, without the absolute valve maintenance of the injector (tokamak), which requires that it is at atmospheric pressure, would require that the tokamak (injector) is also at atmospheric pressure. This is highly undesirable as letting either the tokamak or the injectors up to atmospheric pressure is an operation that will not be rapid and the 'conditioning' of the tokamak and/or the accelerator may be lost.

Also, without the valve any tritium leaking from the tokamak through the shutter into the injector and the NB cell, which could lead to the NB cell having to be classified as a 'red' area, into which man access would be forbidden, making the presently envisaged maintenance schemes untenable.

Because of the neutron and gamma radiation expected from ITER, conventional organic seals deteriorate and lose their mechanical properties, so they cannot be used. Therefore, an all metal valve is mandatory. The use of the fast shutter as described in section 8.1 means that the valve will only be used for maintenance operations, or when the injector concerned is out if use for an extended period, and the number of foreseen open-close operations during the lifetime of ITER is <100, which allows the design to be with zero maintenance. The valve for the ITER injectors has to have a 1.6 m diameter opening which is ≈5 times larger than any existing all metal sealed valve, and ongoing R&D is aimed at qualifying the extrapolation from proven designs.

As mentioned above, the valve will have to be baked *in situ* to comply with the ITER vacuum requirements for all surfaces in direct contact with the ITER vacuum. The foreseen baking system will also act as a cooling system when the valve is closed and the tokamak operating as in that situation the 'gate' is directly heated by radiation from the ITER plasma.

When the injector is operating, re-ionized beam particles (D^+) will impinge on various surfaces of the valve. Although the calculated power densities are low, ≪1 MW m^{-2}, the foreseen long pulse operation means that sensitive surfaces, such as the sealing surfaces in the valve, must be protected, and cooling foreseen. The conceptual design that has been developed uses a telescopic system of cooled, rectangular cross section, protection 'boxes' that are deployed as the valve is opened to cover the valve entrance and exit, and the sealing surfaces. A CAD generated model of the absolute valve is shown as figure 13.

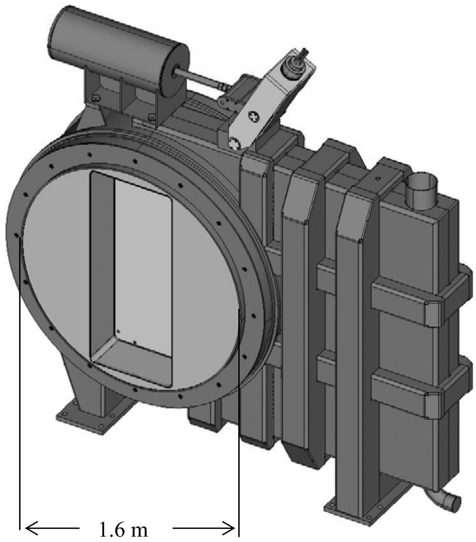

Figure 13. CAD model of the ITER NB all metal sealed gate valve.

8.3. The vacuum vessel suppression system box, the NB drift duct, the NB duct and the NB duct liner

The VVPSS box is located immediately downstream of the absolute valve. The purpose of the VVPSS box is to make the connection between the NB duct and the pipe leading to the VVPSS tanks where the steam, dust etc. from a loss of coolant event inside the tokamak will be collected and condensed. This reduces the maximum overpressure of the tokamak due to the event to <0.15 MPa. (The VVPSS tanks are isolated from the tokamak vaccum by bursting discs which open at <0.15 MPa.) In the present design the NB ducts are the only exits from the tokamak vacuum vessel that are large enough to serve this purpose. The VVPSS box is a large rectangular cross section box with large openings through which the beam passes. The connection to the VVPSS pipe to the suppression tanks consists of a large rectangular, or race track shaped, opening at one side of the injector concerned, that eventually connects to a 1.2 m pipe passing through the NB cell and eventually to the VVPSS suppression tanks. The VVPSS box has to be baked to comply with the ITER tokamak vacuum requirements, and cooled to be able to sustain the expected re-ionization power. The design of the VVPSS box is on going.

The duct downstream of the VVPSS box consists of a first section, the NB drift duct, that incorporates large, double walled, bellows to accommodate dimensional changes and movement due to thermal expansion resulting from the change in temperature of the tokamak when operating. The bellows are protected from any direct beam interception or re-ionized beam particles by a cooled copper screen. The NB drift duct is followed by the NB duct inside of which is the NB duct liner. There is a requirement that the beams can be tilted by ±9 mrad in the vertical plane (see section 6). This leads to a loss of beam in the duct by direct interception of up to ≈0.8 MW, the exact value depending on the accuracy of the beam tilting and the optical characteristics of the beam, particularly the beamlet divergence. This power is intercepted by the duct liner, which prevents any beam directly impinging on the duct walls. Calculations have shown that it is essential to incorporate a small array of thermocouples in critical areas of the liner to ensure safe operation when the beam is tilted.

9. Maintenance

Although the main concept of the ITER injectors has not changed greatly over the past few years, the maintenance scheme has. A change in the organisation of the equipment in the levels above the NB cell allowed the removal of the mezzanine floor and its replacement by a smaller balcony. That allowed access from above to the BLV. Therefore, it was decided to install an overhead crane and adapt the BLV so that the top could be opened (or removed) for access to the beamline components. The chosen solution is a rectangular vessel (see figure 1) with a lid that can be fully opened. However, in order to access the beamline components it was necessary to change the cryopumps from the quasi-cylindrical design that covered the top of the beamline to two flat pumps against the lateral walls of the BLV. Furthermore it became unnecessary to have the components mounted on a rail system; instead they are mounted directly onto supports on the floor of the BLV. Changing a beamline component now involves disconnecting the cooling and instrumentation, lifting the component with the crane which is then used to transport the component to the corner of the NB cell. At that location they are transferred to a trolley, into a cask and then to the hot cell for maintenance or disposal. Replacing the components is the reverse removal. This much simpler maintenance scheme allowed the beamline components to be classified as remote handling class 2, which means that maintenance is expected during the operational life of ITER.

For various reasons the HV bushing still connects to the BSV from above, so the maintenance of the beam source is still ‘horizontal’, i.e. the rear flange on the BSV is opened, coolant, gas, instrumentation and electrical connections are disconnected, the source placed on a trolley in the BSV and the source removed horizontally via the rear of the BSV.

10. Power supplies

The ITER ion source will be held at high negative voltage (−1 MV) and the negative ions will be accelerated up to ground potential. In the 2001 design all the power supplies for the ion source (arc supply, filament supply etc) and the extraction grid were located inside the so-called ‘HV deck’ which was placed on the floor above the NB cell, above the BSV. All the ion source and extraction grid power supplies were referenced to −1 MV and therefore to minimize the size of the HV deck it was filled with SF_6 at 0.6 MPa. Nevertheless, the HV deck was ≈5 m high and ≈5 m in diameter. To minimize maintenance, many of the controls and measurement systems associated with the power supplies in the HV deck were located at ground potential. However, some diagnostics and controls had to be located in the HV deck. For example, the necessity to control individual filament groups in the ion source to attain a sufficient uniformity of illumination of the PG with negative ions would have led to a significant number of control systems inside the HV deck. These considerations led to the decision to locate the ion source and extraction power supplies outside the tokamak building in 'HV deck 1', which is insulated using atmospheric pressure air. In addition to the power supplies for the ion source and extraction grid, the original HV deck also served as an entry point for the cooling water for the ion source and accelerator (high resistance water), the gas for the ion source and the SF_6 and N_2 used for the insulation of the last section of the high voltage transmission line and the high voltage bushing. A new, simplified, 'HV deck 2' has been introduced for these purposes [36], which is very much smaller than the previous HV deck.

11. Summary

Over the past few years the design of the ITER neutral beam system has been refined and new concepts of ion source, maintenance and power system configuration have been adopted, each of which brings significant advantages. Additionally new experiments and developments in calculations of secondary processes in negative ion accelerators have enabled a choice to be made in favour of the MAMuG accelerator concept as opposed to the SINGAP concept, and detailed design calculations have verified the basic concept of subdivided neutralizer and the electrostatic RID. In brief:

- The injector is based on the acceleration of D^- ions to 1 MeV and their neutralization in a gas target. To keep the length of the system reasonable the neutralizer is subdivided into four vertical channels. After neutralization the charged fractions will be removed from the beam using an electrostatic ion dump.
- The ion source chosen is the RF driven ion source as this has achieved good performance, yet needs less maintenance than the filamented source.
- The five stage 1 MeV MAMuG accelerator has been chosen in preference to the SINGAP concept because of the significantly lower electron power that will exit the accelerator, and also because of an apparently better voltage holding ability.
- It has become possible to replace the mezzanine floor in the NB cell with a smaller balcony, which permits the installation of an overhead crane in the NB cell. This opened up the possibility to access the beamline components from above, which enables greatly simplified maintenance of the beamline components. To realize this capability has required changing the BLV shape to have a rectangular cross section with a removable lid and to modify the cryopumps from being quasi-cylindrical to flat rectangular pumps on the side walls of the BCV. It has also been necessary to add an absolute, all metal, gate valve between the injector and the tokamak.
- The BSV shape has been modified to fit to the new BLV shape, and, most importantly, to allow better arrangement of the electrical (high voltage) connections from the bushing to the source and accelerator.
- The SF_6 insulated high voltage deck close to the injectors has been changed to be an air insulated HV deck outside the tokamak building to allow for easier maintenance.

Acknowledgments

Part of this report was prepared as an account of work by or for the ITER Organization. The members of the organization are the People's Republic of China, the European Atomic Energy Community, the Republic of India, Japan, the Republic of Korea, the Russian Federation and the United States of America. The views and opinions expressed herein do not necessarily reflect those of the members or any agency thereof. Dissemination of the information in this paper is governed by the applicable terms of the ITER Joint Implementation Agreement.

References

[1] de Esch H.P.L., Stork D., Challis C. and Tubbing B. 1995 The optimization of neutral beams for ignition and burn *Fusion Eng. Des.* **26** 589–604

[2] Thomas E.W. (ed) 1985 Atomic Data for Fusion. Volume 3: Particle Interactions with Surfaces ORNL 6088 (ORNL-6086 V3) http://www-cfadc.phy.ornl.gov/redbooks/three/d/3d4.html

[3] Oikawa T. *et al* 2008 Benchmarking of neutral beam current drive codes as a basis for the integrated modeling for ITER *Proc. 22nd Int. Conf. on Fusion Energy 2008 (Geneva, Switzerland, 2008)* (Vienna: IAEA) http://www-naweb.iaea.org/napc/physics/FEC/FEC2008/html/index.htm

[4] Krylov A. and Hemsworth R.S. 2006 Gas flow and related beam losses in the ITER neutral beam injector *Fusion Eng. Des.* **81** 2239–48

[5] Fubiani G., de Esch H.P.L., Simonin A. and Hemsworth R.S. 2008 Modeling of secondary emission processes in the negative ion based electrostatic accelerator of the international thermonuclear experimental reactor *Phys. Rev. Special Top.—Accel. Beams* **11** 014202

[6] Fubiani G., Hemsworth R.S. and de Esch H.P.L. 2009 Analysis of the two accelerator concepts foreseen for the neutral beam injector of the international thermonuclear experimental reactor *Phys. Rev. Special Top.—Accel. Beams* submitted

[7] Light T., Licht S., Bevilacqua A. and Norash K. 2005 The fundamental conductivity and resistivity of water *Electrochem. Solid State Lett.* **8** E16–9

[8] McNeely P., Falter H.-D., Fantz U., Franzen P., Fröschle M., Heinemann B., Kraus W., Martens Ch., Riedl R. and Speth E. 2006 Development of a rf negative-ion source for ITER neutral beam injection *Rev. Sci. Instrum.* **77** 03A519

[9] Speth E. *et al* 2006 Overview of the RF source development programme at IPP Garching *Nucl. Fusion* **46** S220–38

[10] Franzen P. *et al* 2008 The IPP RF source: a high power, low pressure negative ion source for the neutral beam injection system of *ITER Int. Conf. on PLASMA-2007 (Greifswald, Germany, October 2007) AIP Conf. Proc.* **993** 51–4

[11] Riz D. and Paméla J. 1998 Modeling of negative ion transport in a plasma source *Rev. Sci. Instrum.* **69** 2

[12] Wünderlich D., Gutser R., Fantz U. and the NNBI Team 2007 Influence of magnetic fields ans biasing on a plasma of a RF driven negative ion source *Proc. 11th Int. Symp. on the Production and Neutralization of Negative Ions and Beams (Santa Fe, USA, September 2006) AIP Conf. Proc.* **925** 46–57

[13] Boilson D., Ellingboe A.R., Faulkner R., Hemsworth R.S., De Esch H.P.L., Krylov A., Massmann P. and Svensson L. 2005 Negative ion yield in long pulse operation of the KAMABOKO III source *Fusion Eng. Des.* **74** 295–8

[14] Boilson D., De Esch H.P.L., Hemsworth R.S., Kashiwagi M., Massmann P. and Svensson L. 2002 Long pulse operation of the KAMABOKO III negative ion source *Rev. Sci. Instrum.* **73** 1093–5

[15] Krylov A., Boilson D., Fantz U., Hemsworth R.S., Provitina O., Pontremoli S. and Zaniol B. 2006 Caesium and tungsten behaviour in the filamented arc driven Kamaboko-III, negative ion source *Nucl. Fusion* **46** S324–31

[16] Kraus W., Berger M., Fantz U., Franzen P., Fröschle M., Heinemann B., Riedl R., Speth E., Stäbler A. and Wünderlich D. 2009 Long pulse H^- beam extraction with a RF driven ion source with low fraction of co-extracted electrons *1st Int. Conf. on Negative Ions, Beams and Sources (Aix-en-Provence, France, 2008) AIP Conf. Proc.* **1097** 275–81

[17] de Esch H.P.L., Hemsworth R.S. and Massmann P. 2005 Updated physics design ITER-SINGAP accelerator *Fusion Eng. Des.* **73** 329

[18] de Esch H.P.L., Svensson L., Inoue T., Taniguchi M., Umeda N. and Kashiwagi M. 2009 Results of the SINGAP neutral beam accelerator experiment at JAEA *1st Int. Conf. on Negative Ions, Beams and Sources (Aix-en-Provence, France, 2008) AIP Conf. Proc.* **1097** 353–63

[19] Taniguchi M., de Esch H.P.L., Svensson L., Umeda N., Kashiwagi M., Watanabe K., Tobari H., Dairaku M., Sakamoto K. and Inoue T. 2009 Development of 1 MeV H^- accelerator at JAEA for ITER NB *1st Int. Conf. on Negative Ions, Beams and Sources (Aix-en-Provence, France, 2008) AIP Conf. Proc.* **1097** 335–43

[20] Cranberg L. 1952 The initiation of electrical breakdown in vacuum *J. Appl. Phys.* **23** 518–22

[21] Charbonnier F.M. 1968 A brief review of vacuum breakdown initiation processes *Proc. 3rd Int. Symp. on Discharges and Electrical Insulation in Vacuum (Paris, France, 1968)* pp 15–34

[22] Williams D.W. and Williams W.T. 1974 Prebreakdown and breakdown characteristics of stainless steel electrodes in vacuum *J. Phys. D: Appl. Phys.* **7** 1173–83

[23] Inoue T. *et al* 2001 Design of neutral beam system for ITER-FEAT *Fusion Eng. Des.* **56–57** 517–21

[24] Grisham L.R. 2007 Lithium jet neutralizer to improve negative hydrogen neutral beam systems *Phys. Plasmas* **14** 102509,1–8

[25] Zhil'tsov V.A., Klimenko E.Yu., Kosarev P.M., Kulygin V.M., Platonov V.V., Semashko N.N., Skovoroda A.A., Ukhov V.P. and Mehed'kin A.A. 2000 The development of a negative ion beam plasma neutralizer for ITER NBI *Nucl. Fusion* **40** 509–13

[26] Chaibi W., Blondel C., Cabaret L., Delsart C., Drag C. and Simonin A. 2009 Photo-neutralization of negative ion beam for future fusion reactor *1st Int. Conf. on Negative Ions, Beams and Sources (Aix-en-Provence, France, 2008) AIP Conf. Proc.* **1097** 385–94

[27] Pamela J. 1986 Gas heating effect in the neutralisers of neutral beam injection lines *Rev. Sci. Instrum.* **56** 1066–9

[28] Hemsworth R.S., Stabler A., Falter H.-D., Massmann P., Deschamps G.H. and Goede A.P.H. 1986 Neutralisation measurements for the JET neutral injectors *Proc. 13th Conf. on Control Fusion and Plasma Heating (Schliersee, FDR, April 1986)* pp 297–300

[29] Ott W. 1989 Beam Heating of the neutraliser gas of neutra lbeam injectors *IPP* 4/237 Max-Planck-Institüt für Plasmaphysik Euratom Association, Garching bei Germany, München

[30] Surrey E., Challis C.D., Ciric D., Cox S.J., Crowley B., Jenkins I., Jones T.T.C. and Keeling D. 2005 Measurement of the depletion of neutraliser target due to gas heating in the JET neutral beam injection system *Fusion Eng. Des.* **73** 141–53

[31] Kamperschroer J.H., Gammel G.M., Kugel H.W., Grisham L.R., Stevenson T.N., von Halle A., Williams M.D. and Jones T.T.C. 1989 Gas utillization in the toakamak fusion test reactor neutral beam injectors *J. Vac. Sci. Technol.* A **7** 83–9

[32] Surrey E. 2006 Gas heating in the neutralizer of the ITER neutral beam injection systems *Nucl. Fusion* **46** S360–8

[33] Surrey E., Holmes A.J.T. and Jones T.T.C. 2009 The effect of beam induced plasma in the ITER electrostatic residual ion dump *1st Int. Conf. on Negative Ions , Beams and Sources (Aix-en-Provence, France, 2008) AIP Conf. Proc* **1097** 402–17

[34] Dremel M., Day Chr., Hemsworth R., Pearce R. and Mayaux C. 2008 Cryopump design for the ITER heating neutral beam injector *Proc. 22nd Int. Conf. on Fusion Energy 2008 (Geneva, Switzerland, 2008)* (Vienna: IAEA) http://www-naweb.iaea.org/napc/physics/FEC/FEC2008/html/index.htm

[35] Dremel M., Day C., Hemsworth R., Pearce R. and Mayaux C. 2008 Cryopump design for the ITER heating neutral beam injector *Nucl. Fusion* submitted

[36] Toigo V., Gaio E. and Milani F. 2005 Comparative analysis of two electric schemes for the ion source power supplies of the neutral beam test bed *21st IEEE/NPSS Symp. on Fusion Engineering (Knoxville, Tennessee, 2005)*